J. Membrane Biol. 136, 253–262 (1993)

The Journal of
Membrane
Biology

A Mechanism for Isotonic Fluid Flow through the Tight Junctions of *Necturus* Gallbladder Epithelium

A.E. Hill, B. Shachar-Hill
Physiological Laboratory, Downing Street, Cambridge CB2 3EG United Kingdom

Received: 17 May 1993/Revised: 27 July 1993

Abstract. During isotonic fluid flow, *Necturus* gallbladder epithelium mediates net fluxes of paracellular probes by a convective process. We show here that the paracellular system is modeled by permeation through three populations of channels: (i) convective parallel-sided ones of width 7.7 nm (ii) small diffusive ones of radius ~0.6 nm, and (ii) large diffusive ones of radius exceeding 50 nm. The reflexion coefficient of the convective channels is very low and the calculated osmotic flow rate is close to zero when compared with the observed fluid absorptive rate of 2×10^{-6} cm/sec. Analysis reveals that the convective channels behave as though closed to back-diffusion of probes; if this is due to solvent drag then very high fluid velocities are required, acting through minute areas. There are no transjunctional gradients that could drive the flow, and so the fluid must be propelled through the channel by components of the junction.

We propose a mechanism based upon an active junctional peristalsis which allows discrimination on the basis of molecular size, in which the channels are always occluded at some point and so back-diffusion cannot occur. There is no local gradient of salt distal to the junctions and therefore the osmotic permeability of the membranes is irrelevant. High fluid velocities are not required, and the flow can occur over a substantial fraction of the junction. The mechanism must involve motile and contractile elements associated with the junction for which there is already considerable evidence.

Key words: Pore sizes — Epithelial junctions — *Necturus* gallbladder — Fluid transport — Convective channels — Reflexion coefficient

Introduction

We have shown in a recent paper, using dextrans as molecular probes, that fluid absorption in *Necturus* gallbladder is a convective process occurring through the junctional pathway (Shachar-Hill & Hill, 1993), and that osmosis cannot account for this flow with the known areas of the junctions and the osmotic permeability of the interspace membranes. Only probes smaller than 7.7 nm can traverse the convection pathway, while at zero probe radius the convective flow is equal to that of the epithelial fluid transfer. In this paper we show that the sizes and frequencies of the paracellular channels responsible for both convective and diffusive fluxes can be calculated from the dextran permeation data. With this information it becomes possible, not only to calculate the reflexion coefficients of the different channels and so assess their contribution to trans-junctional osmosis, but also to put constraints on possible nonosmotic models.

Many studies have been made of the permeability of epithelia to nonelectrolytes, but few are quantitative enough for the sizes or extent of channels to be determined. In a study with nine probes across rabbit gallbladder, van Os, de Jong and Slegers (1974) measured only unidirectional fluxes from mucosal to serosal bath and concluded that there were pores of ~4.0 nm carrying most of the paracellular probe flux. No convective fluxes were measured.

In a study with seven probes, Steward (1982) used a unilateral rabbit gallbladder preparation in which the appearance of the probes in secreted fluid was measured; this differs from the technique where the flux into a relatively large well-stirred bath is measured. Populations of small and large (nondiscriminating) pores were observed, and from the fluxes of the smallest probes it was concluded (correctly, in our view) that a large fraction of the fluid must be crossing the junction. This convection was assigned to the small pores of radius 0.3 nm because no other channels (other than the very large ones) can be revealed by the unilateral flux technique.

Subsequently, using the rabbit submandibular salivary gland, a unilateral preparation, Case et al. (1985) measured fluxes of ten solutes and concluded that there was water and solute flow through channels of width 0.8 nm which could not be explained by pseudo-solvent drag. Whether the route was cellular or paracellular was undecided.

In experiments with *Rhodnius* Malphigian tubule, Whittembury et al. (1986) used nine probes, five of which were true extracellular markers up to dextran MW 15,000. The unilateral secretion showed substantial flow-dependent passage of all the probes, and the authors concluded that they were all subject to paracellular drag of secreted fluid. It should be noted that in *Rhodnius* the interspaces are not thought to be local osmotic coupling spaces; such coupling (if it occurs) is in the microvillous system which would draw water directly out of the luminal cell membrane.

Measurements of the unidirectional fluxes of five solutes from creatinine to inulin MW 5,500 across rat intestine were made by Pappenheimer and Reiss (1987) during conditions of active fluid absorption. The authors concluded, from the results of modulating the transepithelial flows with osmotic gradients, that the junctions contained pores of radius 5.0 nm through which solutes were dragged by convection driven by osmosis.

Experimental Data

The preparation of labeled dextrans, together with the demonstration that they behave as spherical molecular probes, can be found in a recent paper (Shachar-Hill & Hill, 1993), where the flux measurements of these probes across transporting *Necturus* gallbladder with their subsequent fractionation are described, together with details of the estimation of unstirred layers. The resulting fluxes are basically presented as the datapoints in Figs. 1 and 2, where J_{ms}/C_m and J_{sm}/C_s are the unidirectional specific fluxes representing flux per unit area from the mucosal or serosal bath at concentration C_m or C_s, either against or with the absorptive flow which occurs from mucosa to serosa. The difference between these two sets of data are the net fluxes at any radius, defined by

$$J_{net} = J_{ms}/C_m - J_{sm}/C_s \quad (1)$$

and shown as the datapoints in Fig. 3. The net fluxes are statistically highly significant at all probe radii and fit a linear regression with high correlation. The intercept at zero net flow, representing the maximum possible channel width, is 7.7 nm while the flow intercept at zero radius is 2×10^{-6} cm/sec, equal in magnitude to the epithelial fluid flow rate J_v determined previously.

A theoretical analysis in that paper models the combined system of junction, interspace and subepithelium in series, taking account of diffusion-convection coupling in all the elements. It shows that J_{net} is only equal to the epithelial volume flow rate J_v when the probes are confined to the paracellular system and the fluid is all convected through the junction. Osmotic coupling in the interspaces alone accounts for less than 10% of J_{net}.

Analysis and Theory

In this section we analyze the paracellular system as follows. We start from the result that the system must possess 7.7 nm wide channels spanning the junction through which all the fluid passes by an unspecified mode of convection. These are in parallel with diffusion-only channels (Shachar-Hill & Hill, 1993). From the backfluxes (Fig. 2), we show that as the flux of the higher radius probes can be modeled closely by a Stokes-Einstein relationship with no drag, they are traversing very large diffusive pores of unspecified size. We then fit the very steep data at low radii to small diffusion-only pores in parallel; the shape of these is undetermined but either parallel or cylindrical channels show very similar dimensions.

Above the radii of the small channels, the forward and backward flux data (Figs. 1 and 2) must represent flow through both the large diffusive channels (of total area A_b) in parallel with the 7.7 nm convective channels. In the latter, simple convection-diffusion is initially assumed to occur with velocity v between parallel walls, described by Eq. (2); a fit to parallel-walled channels is chosen because the net fluxes are linear with probe radius (Fig. 3) and only this geometry can generate linearity (*see next section*). A_b and v are extracted as fitted parameters. The value of v is then considered in relation to fluid flow by trans-junctional osmosis and other mechanisms. It appears that v is so high that it is impossible it could be generated by any forces requiring hydraulic flow, and other mechanisms must be considered.

In any determination of the fraction of the junctional area occupied by diffusive channels, the junction length L is an important parameter. However, the sizes of the channels are not dependent upon L but are determined from curve fits as a variable separate from A/L. All the area fractions which appear in the Table are therefore referred to a similar L. In the case of convective flow calculations in

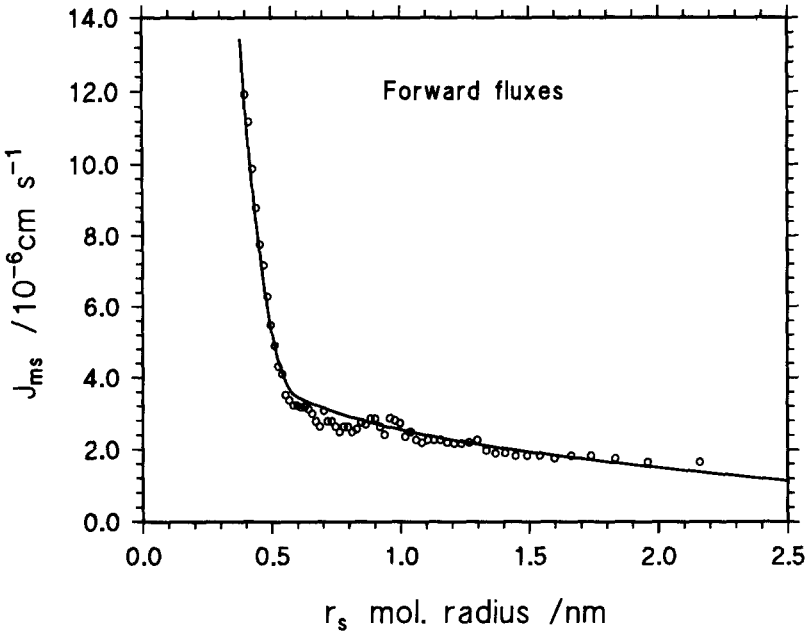

Fig. 1. Probe fluxes (mucosa to serosa) as a function of molecular radius fitted by Eq. (11).

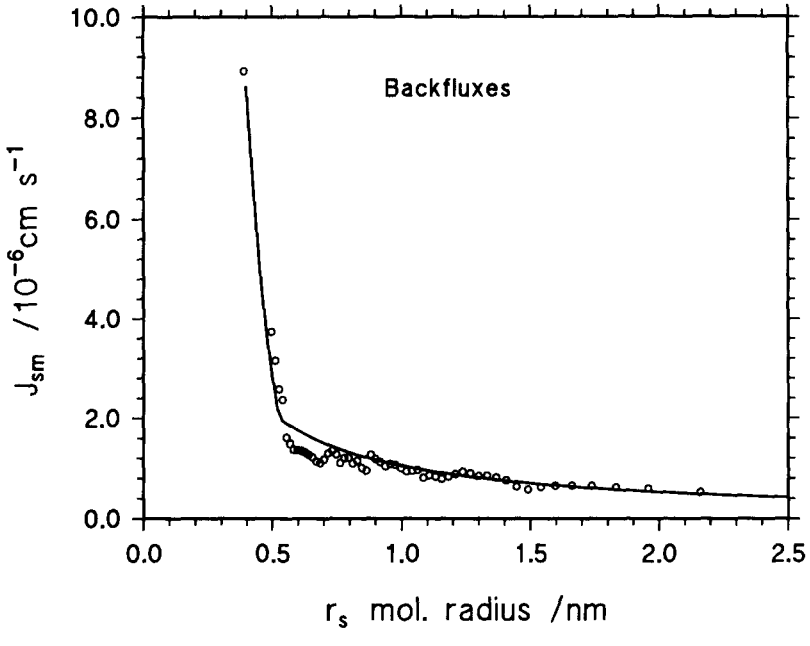

Fig. 2. Probe backfluxes (serosa to mucosa) as a function of molecular radius fitted by Eq. (12).

the channel, L plays no part because A_c is derived reciprocally from the total volume flow, vA_c, after calculating the velocity v.

Steric and Drag Factors

The flux by convection-diffusion through a channel between two baths is given by the general equation

$$J_{ij} = vAGS_f \frac{C_i \exp(vGS_fL/DFS_d) - C_j}{\exp(vGS_fL/DFS_d) - 1}. \quad (2)$$

In the calculations, the steric factors S and the drag factors F and G, by which mobilities depart from their free solution values when confined to narrow channels, play an important part. These are derived from hydrodynamic theory (Renkin & Curry, 1979). We have used the expressions for diffusive and convective drag factors in circular channels

$$F = 1 - 2.1019\lambda + 2.05829\lambda^3 - 1.6764\lambda^5 + 0.6772\lambda^6 \quad (3)$$

and

$$G = 1 - 0.66236\lambda^2 - 0.08335\lambda^3 + 0.25462\lambda^4 \quad (4)$$

which are polynomials fitted to the computed results of Wang and Skalak (1969) where $\lambda = r_s/r_{\text{channel}}$. For parallel channels, similar fits have been made to the expressions of Faxen (1922) for "radially averaged" solutions

$$F = 1 - 1.868\lambda + 3.462\lambda^2 - 3.39\lambda^3 + 0.064\lambda^4 + 0.709\lambda^5. \quad (5)$$

and Wayika (1957)

$$G = 1 - 0.022\lambda - 0.1102\lambda^2 - 2.8367\lambda^3. \quad (6)$$

The steric factors depend upon the flow regime in the channel. For diffusion, S_d represents the ratio of the solute concentration per unit volume of the channel to that of the bath; due to the probes having a finite radius this is less than 1.0. It is given on simple geometric grounds by $(1 - \lambda)$ for parallel-sided channels or $(1 - \lambda)^2$ for circular pores. In the convective case, the factor S_f is more complex because the fluid velocity and solute concentration both vary with distance from the channel wall. The treatment of Ferry (1936), used as the basis of capillary permeability by Pappenheimer, Renkin and Borrero (1951), calculates S_f by assuming that the solutes follow streamlines and by ignoring G. Fortunately, in the final analysis when fits are made to the net fluxes in Fig. 3, the linearity of the data demands that $G = 1$, in which case $S_f = S_d$. Interim calculations on drag in the convective channels were initially made with the expression for Poiseuille flow in a parallel channel $S_f = 1 - 3\lambda/2 + \lambda^3/2$ (Renkin & Curry, 1979), but the results (that enormous fluid velocities are required in these channels if free diffusion is possible) are quite insensitive to the precise expression for S_f and so one factor equal to $(1 - \lambda)$ was finally used throughout.

If junctional convection is driven by any transjunctional force (osmotic, electro-osmotic or hydrostatic), the probes must experience drag with the channel walls and the convective drag factor should be less than 1.0. In the apparent absence of such forces, the fluid must be impelled by the movement of a component of the channel wall itself. This has direct implications both for the drag coefficient G and the geometry. Only for parallel-walled channels with $G = 1$ is the convective flux $vAGS$ (*see* Eq. 11) a linear function of probe radius as found experimentally (Fig. 3).

Size and Area of Diffusive Channels

The steepness of the rise in backflux at a small probe radius requires a population of small channels with a cutoff at about $r_s = 0.6$ nm. The points above this radius show a weak dependency on r_s which indicates a large channel in which steric effects or diffusional drag play little part. These latter points have been fitted to the diffusive equation

$$\frac{J_{sm}}{C_s} = D(A_b/L) = \frac{RT(A_b/L)}{6\pi r_s \eta_w N} \quad (7)$$

where A_b/L is the total channel area to length ratio, the diffusion coefficient D is given by the Stokes-Einstein relationship, and the dynamic viscosity of water η_w is $10^{-9}\ J \cdot s/\text{cm}^3$ at 20°. There is no calculation of the steric or diffusional drag coefficients S and F applicable to such a channel (*see below*) because Eq. (7) represents diffusion in free solution or through a very large channel in which S and $F = 1.0$.

Equation (7) represents the flattest curve that could be drawn for any diffusional channel: a smaller channel, or any combination of such channels, would in its form show a steeper dependence on probe radius than one based upon free diffusion values for D. The equation has been fitted to the backflux data above 0.7 nm in Fig. 2 by a routine which adjusts A_b/L as the variable. The fit is very close, as can be seen in the right-hand part of the figure, indicating that above about 0.7 nm only large channels are present within experimental error. There may be a small contribution of the convective channels to these data points (*but see next section*). The value of A_b/L required is ~0.45. With a junction depth L of 0.4 μm, A_b is equal to 3×10^{-5} cm^2 per cm^2 epithelium, assuming that these large channels reside in the junction. If the junctional width d is 8.0 nm, and its linear extent l in the epithelial plane is 1,300 cm/cm^2, the area fraction A_b/dl comes out at 2.9×10^{-2}, i.e., 3% of the available junction area (Table). These may be parallel channels or pores, representing structural elements of the junction or the combined effect of leak pathways. The electrical conductivity g of this pathway is equal to $\kappa A_b/L$ and when filled with 100 mM NaCl, the specific conductivity κ of which is 1.0×10^{-2} S/cm, its value is 4.5 mS per cm^2 epithelium. The conductivity of *Necturus* gallbladder epithelium is ~10–14 mS/cm^2 and so the large channels should contribute about a third to the "leakiness" of this tissue. It seems likely that they are a distributed element of the paracellular pathway and not artifacts because the mounting cassette is designed to minimize edge damage. The variation is quite small between the tissue fluxes at large radii.

The permeability at small radii can be modeled either as parallel-sided channels or circular pores and in both cases reasonable fits are obtained. In Fig. 2 a fit to the data is shown (Eq. 12) using 0.6 nm radius pores with an A_s/L value of 10.0 in parallel

with the large channels. The extreme steepness of the data at low radii means that a variety of channel dimensions and areas can be fitted, but acceptable fits all lie between 0.55–0.7 nm half-width or radius. It is difficult to predict the precise effect these small channels will have on the electrical conductivity because they may be charged, but it is possible to extrapolate from the experimental data because the first six datapoints of Fig. 2 fit a linear regression line $J_{sm}/C_s = [-44.8\ r_s + 26.26] \times 10^{-6}$ with a correlation coefficient of −0.99. At 0.2 nm radius, approximately that of a small hydrated ion, the partial relative flux J_{sm}/C_s is 17.3×10^{-6} cm/sec. Using the partial conductance relation for an ion (Hodgkin, 1951) under conditions of short-circuit flux

$$g_{\text{ion}} = \frac{F^2}{RT}(J_{sm}/C_s)C_{\text{bath}} \tag{8}$$

and $C_{\text{bath}} = 0.1 \times 10^{-3}$ mol/cm^3 for *Necturus* saline, we obtain a partial conductance of 6.5 mS, or 13 mS overall conductance of the tissue for cations and anions if both can freely enter the pores. Comparison with the measured value of 10–14 mS/cm^2 for the epithelium indicates that, on grounds of permeation according to size alone, the dextran flux values are in reasonable agreement with electrical measurements.

It thus appears that at most one-third of the *Necturus* gallbladder conductance is due to large nondiscriminating channels and at least two-thirds to small channels of approximate width 0.6 nm. These fractions, however approximate, do indicate that a significant contribution to the high conductivity of such a "leaky epithelium" as *Necturus* gallbladder is made by small channels which are not indiscriminate leak pathways but part of the junctional architecture.

Size and Area of Convective Channels

A participation of the convective channels in diffusive transfer is not apparent from the fit to the backfluxes shown in Fig. 2, comprising only the small and large diffusive channels (Eq. 12). However, the contribution of the convective channels may easily be estimated by extending the fitting routine to include them in parallel. Applying Eq. (2) with $S_f = S_d$ to the paracellular pathway above 0.7 nm radius, which evades the small channels, the fluxes are given by

$$\frac{J_{ms}}{C_m} = vA_cG_cS_c\frac{\exp(vG_cL/DF_c)}{\exp(vG_cL/DF_c) - 1} + \frac{DA_b}{L} \tag{9}$$

and

$$\frac{J_{sm}}{C_s} = vA_cG_cS_c\frac{1}{\exp(vG_cL/DF_c) - 1} + \frac{DA_b}{L} \tag{10}$$

where the first r.h.s. (exponential) terms represent transport through the convective channel with the appropriate diffusive and convective drag factors F_c and G_c, and the steric factor S_c for parallel-sided channels. The second r.h.s. term, which is the same in each direction, is the diffusion through the large channels as given by Eq. (7). L is the junction length and A_c and A_b are the cross-sections of the convective and the large diffusional channels. The fluid velocity in the convective channel is v.

A nonlinear curve-fitting routine by the method of Marquardt was used to fit the data with v and A_b/L as variable parameters. Equation (9) was fitted to the forward flux data of Fig. 1 and Eq. (10) to the backflux data of Fig. 2. vA_c is the total fluid convective velocity through the paracellular pathway equal to 2.02×10^{-6} cm/sec. For each probe, radius D was calculated from the Stokes-Einstein relationship ($D = RT/6\pi r_s\eta_w N$) and F_c and G_c were given by the expressions for a parallel channel, Eqs. (5) and (6), with S_c equal to $(1 - \lambda)$. The results indicate quite clearly that the value of v required is very large, in excess of 1,000 cm/sec, so that the exponential terms are enormous; the $m - s$ flux through the convective channel in Eq. (9) can therefore be equated to vA_cS_c while the $s - m$ flux through the convective channel in Eq. (10) collapses to zero. The term A_b/L comes out to be 0.435 and 0.453 (±0.01) from Eqs. (9) and (10), in good agreement with each other.

The convective channels of 7.7 nm radius behave, therefore, as effectively "convection-only" pathways under normal conditions of isotonic absorption, and the backflux through these convective channels is negligible. If the flows are due to fluid convection alone, the flow rate must be high enough to reduce the probe backflux to a value that is indistinguishable from zero. We can therefore write the overall equations for permeation without any loss of accuracy as

$$\frac{J_{ms}}{C_m} = vA_cG_cS_c + \frac{DA_b}{L} + \frac{DA_sF_sS_s}{L} \tag{11}$$

and

$$\frac{J_{sm}}{C_s} = \frac{DA_b}{L} + \frac{DA_sF_sS_s}{L} \tag{12}$$

in which the small channels of area A_s have been added with their respective steric and diffusive drag factors. Equivalent factors for the large channels are not shown because they are equal to 1.0. These are

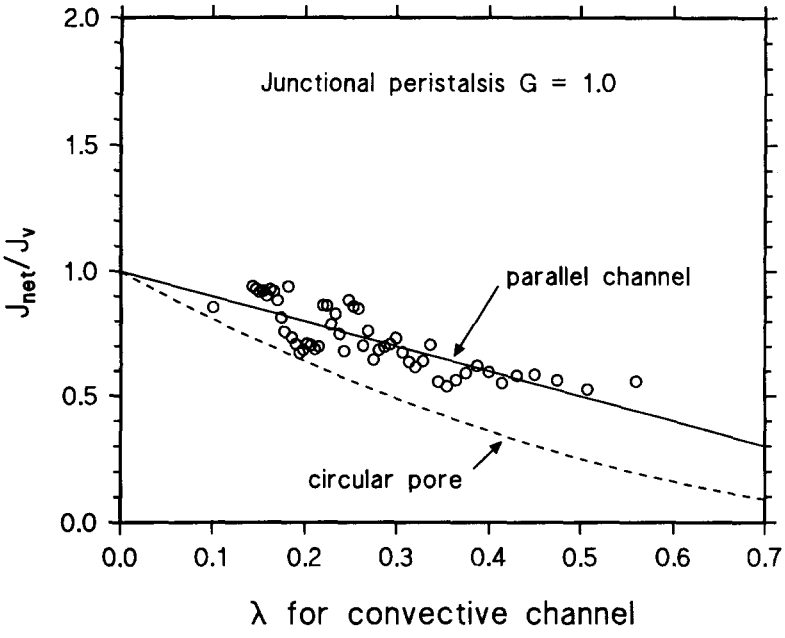

Fig. 3. Net probe fluxes J_{net} as a fraction of the epithelial fluid flow rate J_v (2×10^{-6} cm/sec) plotted against λ the ratio of probe radius r_s to channel half-width r_c (7.7 nm). The curves are plots of J_{net} calculated from Eqs. (1) and (11–12) using the junctional channel data evalulated in this paper. They are identical to those derived in the previous paper (Shachar-Hill & Hill, 1993) for the junctional convection model which comprises junction, interspace and subepithelium in series, indicating that apart from the junction the other components exert little discrimination between different solutes and water. (i) Dotted line: peristaltic channel flow through circular pores 7.7 nm diameter with diffusion through the large and small channels; (ii) unbroken line: peristaltic channel flow through parallel-sided channels 7.7 nm wide with diffusion through the large and small channels. The straight-line fit, which is identical to the regression line, is equivalent to the curve for the steric coefficient given by $S_c = (1 - \lambda)$, indicating that parallel channels are involved. For peristaltic flow $G = 1$ at all radii.

good fits to the unidirectional fluxes and Eq. (11) represents the curve in Fig. 1, Eq. (12) that in Fig. 2.

If the convective flow is through open channels as assumed in Eqs. (11) and (12), the area occupied by the convective channels can be calculated from v and the overall convective flow through the channels vA_c (2×10^{-6} cm/sec). For v = 1,000 cm/sec, the area A_c is 2×10^{-9} cm^2 per cm^2 epithelium, a value which is exceptionally small, equal to 0.0002% of the junctional cross section (10^{-3}). It must be clear at this stage that this calculation is purely an academic exercise and there are no forces operating that could produce such enormous flow rates through such minute areas. The conclusion must be that the net flux is not described by simple convection-diffusion theory applied to open channels.

Trans-Junctional Osmosis

The reflexion coefficient of a channel is given by osmotic theory (Mason & Viehland, 1978; Castillo & Mason, 1980; Hill, 1989) as

$$\sigma = \theta\left(1 - \frac{D_s V_s}{D_w V_w} - \frac{D_s}{D_s^0}\right) \tag{13}$$

where θ is the diffusive/pressure-driven flow ratio

$$\theta = \left(1 + \frac{Bx^2RT}{\eta_w D_w V_w}\right)^{-1}. \tag{14}$$

B is a constant dependent upon the geometry equal to $\frac{1}{8}$ for cylindrical pores (x = radius) or $\frac{1}{12}$ for parallel channels (x = separation).[1] In Eqs. (13) and (14), the diffusion coefficients D_s and D_w are the values for the channel core and must therefore be calculated from the free-solution values, D_s^o and D_w^o, modified by the steric and drag factors S and F. The osmotic flow through a channel is equal to $\sigma\, qL_pD_pD_p\Delta\pi$, where q is the area fraction available for the channels, L_p is their hydraulic conductivity and $\Delta\pi$ is the osmotic driving force. For the 7.7 nm convective channels, which are parallel sided, the value of L_p is equivalent to 3.38×10^{-3} cm/sec · osmolar (Shachar-Hill & Hill, 1993). By Eq. (13) the

[1] The expression $\sigma = 1 - \frac{A_s}{A_w}$ which is extensively used, where A_s and A_w are the "available filtration areas" for solute and water, we regard as incorrect. However, the use of this traditional formula also leads to values of σ which are very low.

Table. Channel parameters from the permeation data

Channel (shape)	Transfer mechanism	r_c (nm)	Area of epithelium (cm^2/cm^2)	Area of junction (%)	g (mS/cm)	σ
Small (unspecified)	Diffusion	0.55–0.7	$1–4 \times 10^{-4}$	10–40	13	0.003–0.007
Large (unspecified)	Diffusion	>50	3×10^{-5}	3	4	0.0
Convective (parallel walls)	Convection	3.85	2×10^{-8}	0.0002	~0	0.002
	Peristalsis	3.85	$<8.8 \times 10^{-4}$	88 max	0	0

The dimension r_c represents the radius of a pore or half-width of a parallel channel: the small and large channels can be fitted by either. The reflexion coefficients σ are calculated for small ions of 0.2 nm radius.

reflexion coefficient σ for ions (~0.2 nm radius) is −0.002. This is predicted because the channel is so leaky that there is virtually no osmotic flow except the back leakage of salt. Taking into account the minute value of q determined above (0.0002%) and the maximum detected driving force due to intercellular salt of 0.002 osmolar (Ikonomov, Simon & Fromter, 1985), it becomes clear that the osmotic flow rate through these channels is so small ($<10^{-12}$) by comparison with the 2×10^{-6} cm/sec observed, that it can be taken as zero. This is a confirmation of the result reached previously that the junctional convection cannot be an osmotic flow.

Similar calculations for the large indiscriminate channels and the small radius channels give flow rates close to 0 and 5% of that observed, although neither of these channels contributes to the convective flow. It is clear from the fact that the net flux J_{net} does not fall abruptly at a probe radius approaching 0.6 nm (Fig. 3) that there is no detectable convective flow through the small channels within experimental error. It also indicates that there can be little (if any) hyperosmolarity in the interspaces: if there were 10 mOs, for example, the expected flow rate would be 20% of the absorption and would be detectable as a rise in J_{net} at small radii.

In this context it is important to consider the assumption of Pappenheimer and Reiss (1987) that junctional convection is occurring by osmosis through 5.0 nm pores. These authors did not calculate the reflexion coefficient for small ions or metabolites such as glucose, but had they done so it would be apparent that σ of the pores would be close to zero. Moreover, under these conditions the net flux of solute is out of the interspace back to the mucosal bath. The volume flow, calculated from the junctional areas, and assuming an interspace hyperosmolarity of a few mOs, can only account for a minute fraction of the fluid absorption rate. Although widening of trans-junctional channels may occur during the response to luminal sugars, this cannot by itself account for any increases in solvent drag but would rather lower uptake by decreasing σ.

To sum up this section, it must be clear that there can be no detectable osmotic flow in *Necturus* that could be driven by a gradient of salt small enough to escape detection by microelectrodes, through any of the three channels spanning the junction (Table). The convective channels, which mediate a flow equal in magnitude to the fluid absorption rate by the epithelium, cannot be considered to be the pathways of fluid production driven by salt gradients between the apical bath and the interspaces. Even if this were feasible, it would still leave unsolved the problem that all the volume flow apparently occurs through the junctions. The cell membranes must apparently contribute little to the fluid production, a fact that is not compatible with their osmotic permeability. Nor is there any other gradient operating across the junctions that could cause the flow. If there are any slight differences of hydrostatic pressure between interspace and apical bath, they would be such as to drive fluid back out of the junction: the pressure in the interspace must be raised above that of the baths if they are not to collapse. Gradients of electrical potential are very small in *Necturus* gallbladder epithelium (the open circuit potential is 0.5 mV) and the volume flow is unresponsive to small changes in the transepithelial PD, which indicates that electro-osmosis can play little if any part.

Models for Junctional Convection

We propose that there is no measurable hyperosmolarity in the interspaces and that the fluid is driven across the epithelium, probably *via* the junctions, by mechanical action. The junctional complex is a dynamic organelle and not a passive structure medi-

ating only diffusion or osmosis. The driving force is provided directly by cellular free energy, either from chemical intermediates such as ATP, or from the ionic gradients of Na^+ and K^+ built up by the cell. It is possible to choose between three different mechanisms that could be in operation, shown in Fig. 4.

Membrane Drag

The membrane, or components within it, may move the length of the junction and transfer momentum to the fluid with respect to the baths; we call this membrane drag (Fig. 4*A*). The channel is then open for convection and diffusion, and possesses a definite hydraulic and electrical conductivity. There is, however, the question of the fluid flow rate in the channels. The required velocity is so great as to rule out any possible mechanism that could be operative within the adjacent cytoplasm. One of the fastest known relative velocities between cellular components is that between actin and myosin in striated muscle, which may be as great as 20 μm/sec but which is still insignificant by comparison with the velocities required for membrane drag; we do not consider this mechanism any further.

Junctional Peristalsis

If there is closure of the channel at some points (nexus) followed by movement of the nexus along the junction, this is a form of peristalsis (Fig. 4*B*). If there is always at least one nexus present in any channel section at any time, then the mechanism involves the following properties:

(i) The channel acts as a volume pump transferring water, ions and molecules, whose fluxes are determined either by the sieving properties of elements in series with the peristaltic mechanism or by its width through the steric diffusion factor S_c. If the channel loads with solutes in accordance with S_c, the net solute fluxes should show the linear dependence on probe radius expected from this factor. For parallel-sided channels $S_c = 1 - \lambda$, and it can be seen from Fig. 3 that this is indeed the case. This is in accord with the known structure of these junctions which contain parallel membranes spaced 6.0–8.0 nm apart (Hill & Hill, 1978).

(ii) There is no apparent diffusion or electrical conductance through the channel that could be measured across the epithelium because of the nexus. This explains why the convective channels are apparently not permeated by probe molecules from the serosal side. Electrically, the combined conductance of the diffusive channels accounts for the overall conductance and no additional contribution is required.

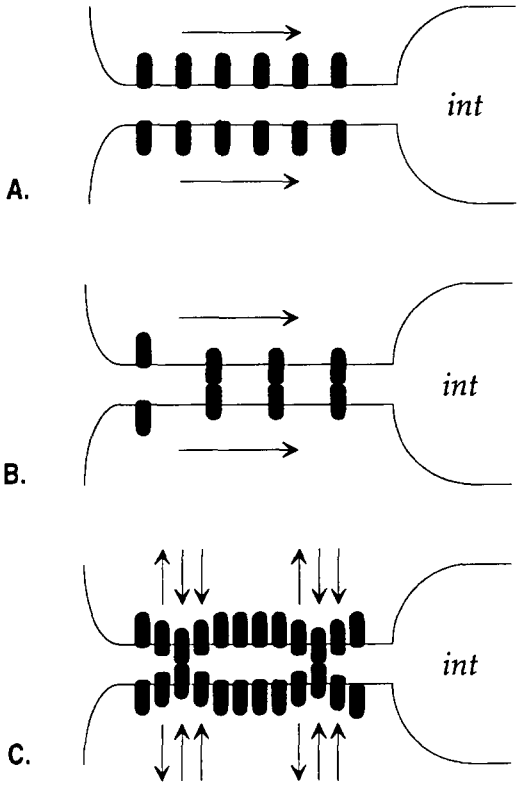

Fig. 4. Three models of convective flow driven by junctional components. (*A*) Membrane drag: mobile components traverse the length of the junctional membrane and the channel fluid experiences drag originating from the wall. (*B*) Forced convection by longitudinal movement: mobile components traverse the membrane as in *A*, but with channel closure (nexus). (*C*) Peristalsis with transverse movements: small lateral movements open or constrict the channel as a wave.

(iii) The apparent convective drag factor G will be 1.0 for all solutes. This follows from the fact that although the channel will fill according to S_c depending on the probe radius, there will be no discrimination by the flow mechanism in respect to radius once molecules have entered the channel.

(iv) There will be no need for high fluid velocities because the only constraint on v is now that determined by the fluid flow $v = J_v/A_c$: the minimum value, if all the area of the junction were available, would be 20 μm/sec. However, it is still unlikely that any component could longitudinally traverse the membrane lining the junction at this speed and the velocity could be a peristaltic wave velocity in which junctional elements execute only relatively small lateral movements (Fig. 4*C*). This would remove the need to recycle the components between apical and basal membranes allowing them to remain *in situ* without ploughing through the membrane.

Leaky Junction Structure

If the junctional complexes are involved in producing volume flow, then the components of the mechanism required must be present in the adjacent cytoplasmic region associated with the junctions, although it is not yet clear how they are organized. We think it possible that the strands of the *zonula occludens* may comprise part of the closure mechanism and that the anastomosis of the strands organizes it into adjacent "domains." Peristaltic closure would thus proceed on a localized basis rather than have to be coordinated simultaneously around the whole cell perimeter. If this is so, then the spaces between the particles comprising the strands would behave as shunt paths of small radius in parallel with (although traversing) the peristaltic mechanism, as observed in the present study.

The dynamic nature of junctional structures has been elegantly demonstrated in the process of extrusion of intestinal cells at the top of the villus in vivo (Madara, 1990). It may prove significant that there is a specialization along the complex in the distribution of actin, myosin, actin-linked proteins and the newly discovered ZO-1 and cingulin. It has also been shown that the appearance of the tight junctions and the actin-myosin ring around the *zonula adherens* show changes in arrangement accompanying alteration in the state of the transport mechanism (Madara & Pappenheimer, 1987; Madara, 1992). Clearly, further information on the precise organization of the complex will complement the transport studies.

Relation to Ion Transport

From previous work with *Necturus* gallbladder epithelium, it is apparent that the combination of Na pumping with concomitant electrodiffusive gradients is not sufficient to account for the net salt flux and, therefore, another mechanism for transfer must be operating.

The Na pump rate during isotonic transport can be measured by two different methods which gave similar values (Hill & Hill, 1987*b*). (i) The fraction of basolateral tracer Na efflux from the cellular compartment that is inhibited by ouabain, taken to be the pump, was only 36% of the transepithelial rate; this was in spite of the fact that ouabain can be shown to fill the interspace compartment very quickly and bind to the Na pump with normal binding constants. (ii) The initial rate of rise of cytosolic Na after ouabain treatment (d[Na]/dt; $t = 0$), which should also equal the pump rate, can be measured in two ways: by Na microelectrodes, and by the rise of tracer Na in the cellular compartment. These gave very similar values of 32 and 35% of the transepithelial rate. Similar values are obtained from microelectrode studies on *Necturus* gallbladder by other workers (Jensen, Fisher & Spring, 1984; Weinman & Reuss, 1984; *see analysis* in Hill & Hill, 1987*b*).

Compartmental analysis of the steady-state Cl fluxes shows that only 15% of the Cl flux traverses the cell. In addition, there are no electrodiffusive driving forces that could account for more than 10% of the absorptive Cl flux through the paracellular pathway (Hill & Hill, 1987*a*).

It thus seems clear that local osmosis based upon the Na pump is ruled out on these grounds and that a paracellular mechanism is required to transport most of the salt. Junctional peristalsis would transfer both volume and ions, and its coordination with the cellular transport mechanisms needs to be investigated.

Symbols

A_i	filtration area of channel i; $i = b$ (big), s (small) and c (convectional)
B	constant for streamline flow
C_i	concentration of probe at i
D	diffusion coefficient
D^0	diffusion coefficient in free solution
d	width of junction
F_i	diffusive drag factor in channel i
g	ionic conductivity
G_i	convective drag factor in channel i
J_{ij}	probe flux from i to j
J_{net}	net probe flux
J_v	volume flow per cm^2 of epithelium
l	linear extent of junction per cm^2 epithelial plane
L	length of junctional channel
L_p	hydraulic conductivity
N	Avogadro's number
q	available filtration area fraction of channel
r_s	probe molecular radius
r_c	channel radius or half-width
S_i	steric factor in channel i
$V_{w,s}$	partial molar volume of water or salt
v_i	fluid velocity in channel i
η_w	dynamic viscosity of water
κ	specific conductivity
λ	ratio of solute radius to channel radius or half-width
θ	diffusive/pressure-driven flow ratio
σ	reflexion coefficient

References

Case, R.M., Cook, D.I., Hunter, M., Steward, M.C., Young, J.A. 1985. Transepithelial transport of nonelectrolytes in the

rabbit mandibular salivary gland. *J. Membrane Biol.* **84:** 239–248

Castillo, L.F., Mason, E.A. 1980. Statistical-mechanical theory of passive transport through partially sieving or leaky membranes. *Biophys. Chem.* **12:**223–233

Faxen, H. 1922. Der Widerstand gegen die Bewegung einer starren Kugel in einer zahen Flussigkeit, die zwischen zwei parallelen ebenen Wanden eingeschlossen ist. *Annal. der Physik* **68:**89–119

Ferry, J.D. 1936. Statistical evaluation of sieve constants in ultrafiltration. *J. Gen. Physiol.* **20:**95–104

Hill, A.E. 1981. Junctional flows of salt and water: towards a unified theory of fluid transfer. *In:* Water Transport Across Epithelia. Alfred Benzon Symposium 15. H.H. Ussing *et al.*, editors. Munksgaard, Copenhagen

Hill, A.E. 1989. Osmotic flow equations for leaky porous membranes. *Proc. R. Soc. London B.* **237:**369–377

Hill, A.E., Hill, B.S. 1978. Sucrose fluxes and junctional water flow across *Necturus* gall-bladder epithelium. *Proc. R. Soc. London B* **200:**163–174

Hill, A.E., Hill, B.S. 1987*a*. Steady-state analysis of ion fluxes in *Necturus* gall-bladder epithelial cells. *J. Physiol.* **382:**15–34

Hill, B.S., Hill, A.E. 1987*b*. Transcellular sodium fluxes and pump activity in *Necturus* gall-bladder epithelial cells. *J. Physiol.* **382:**35–49

Hodgkin, A.L. 1951. The ionic basis of electrical activity in nerve and muscle. *Biol. Rev.* **26:**339–409

Ikonomov, O., Simon, M., Fromter, E. 1985. Electrophysiological studies on lateral intercellular spaces of *Necturus* gallbladder epithelium. *Pfluegers Arch.* **403:**301–307

Jensen, P.K., Fisher, R.S., Spring, K.R. 1984. Feedback inhibition of NaCl entry in *Necturus* gallbladder epithelial cells. *J. Membrane Biol.* **82:**95–104

Madara, J.L. 1990. Maintenance of the macromolecular barrier at cell extrusion sites in intestinal epithelium: physiological rearrangement of tight junction. *J. Membrane Biol.* **116:** 177–184

Madara, J.L. 1992. Anatomy of the tight junction: vertebrates. *In:* Tight Junctions. M. Cereijido, editor. CRC, Ann Arbor, MI

Madara, J.L., Pappenheimer, J.R. 1987. Structural basis for physiological regulation of paracellular pathways in intestinal epithelia. *J. Membrane Biol.* **100:**149–164

Mason, E.A., Viehland, L.A. 1978. Statistical-mechanical theory of membrane transport for multicomponent systems: passive transport through open membranes. *J. Chem. Phys.* **68:** 3562–3573

Pappenheimer, J.R., Reiss, K.Z. 1987. Contribution of solvent drag through intercellular junctions to absorption of nutrients by the small intestine of the rat. *J. Membrane Biol.* **100:**123–136

Pappenheimer, J.R., Renkin, E.M., Borrero, L.M. 1951. Filtration, diffusion and molecular sieving through peripheral capillary membranes. A contribution to the pore theory of capillary permeability. *Am. J. Physiol.* **167:**13–46

Renkin, E.M., Curry, F.E. 1979. Transport of water and solutes across capillary endothelium. *In:* Membrane Transport in Biology. G. Giebisch, D.C. Tosteson, H.H. Ussing, editors. Vol. IVA, Chapter 1. Springer-Verlag, New York

Shachar-Hill, B., Hill, A.E. 1993. Convective fluid flow through the paracellular system of *Necturus* gallbladder epithelium as revealed by dextran probes. *J. Physiol.* **468:**463–486

Steward, M. 1982. Paracellular non-electrolyte permeation during fluid transport across rabbit gall-bladder epithelium. *J. Physiol.* **322:**419–439

Van Os, C.H., De Jong, M.D., Slegers, F.G. 1974. Dimensions of polar pathways through rabbit gallbladder epithelium. *J. Membrane Biol.* **15:**363–382

Wang, H., Skalak, R. 1969. Viscous flow in a cylindrical tube containing a line of spherical particles. *J. Fluid Mech.* **38:**75–96

Wayika, S. 1957. Viscous flows past a spheroid. *J. Phys. Soc. Japan* **12:**1130–1141

Weinman, S.A., Reuss, L. 1984. Na-H exchange and Na entry across the apical membrane of *Necturus* gallbladder. *J. Gen. Physiol.* **83:**57–74

Whittembury, G., Biondi, A.C., Paz-Aliaga, A., Linares, H., Parthe, V., Linares, N. 1986. Transcellular and paracellular flow of water during secretion in the upper segment of the malpighian tubule of *Rhodnius prolixus:* solvent drag of molecules of graded size. *J. Exp. Biol.* **123:**71–92